https://doi.org/10.1595/205651324X17042087562424 *Johnson Matthey Technol. Rev.*, 2024, **68**, (2), 201–211

JOHNSON MATTHEY
TECHNOLOGY REVIEW

technology.matthey.com

The Effect of Platinum Single Atoms in Titania for Photocatalytic Applications

Water oxidation and photocatalytic hydrogen evolution reaction

C. A. G. Bezerra, D. Mamedov, N. Alonso-Vante*
IC2MP, UMR-CNRS 7285, University of Poitiers, F-86022 Poitiers Cedex, France

***Email:** nicolas.alonso.vante@univ-poitiers.fr

PEER REVIEWED

Received 26th June 2023; Revised 4th September 2023; Accepted 14th September 2023; Online xxx MMM 2024

The photocatalytic effect of titania has long been studied with respect to water oxidation and hydrogen evolution. At present, the modification of this semiconducting material by platinum single atoms (Pt-SAs) represents an interesting approach that has been developed in the past decade and has given good results in the photocatalytic hydrogen evolution reaction (HER). Experimental studies have shown that the deposition of Pt-SAs on the titania surface, in aqueous systems, is a spontaneous process and can also be promoted by different reducing processes. Theoretical studies suggest that this deposition is a site-specific reaction, which occurs in oxygen vacancies on the titania surface. Under such conditions, the Pt-SAs are not in a metallic state, due to the interaction with neighbouring atoms of the substrate. This complex system can be probed using different advanced characterisation techniques, which provide a deeper understanding about the modified surface and how this modification improves the photocatalytic performance of titania.

1. Introduction

Growing concern about climate change has prompted a concerted research effort in many parts of the world in search of environmentally friendly and more sustainable energy resources. One of the most active areas in this field is the photocatalytic generation of hydrogen from water splitting, promoted by the generation of electron-hole pairs in semiconductor materials (1).

Among the semiconductors used to promote the water splitting process, titania is one of the most investigated materials (2) due to its physicochemical properties and the fact that this material is an inexpensive and very abundant oxide. Titania is an n-type semiconductor, being non-toxic and relatively stable in acidic and alkaline media (3). But due to its broad band gap energy (3.2 eV for the anatase crystalline structure (4)) titania absorbs light in the ultraviolet (UV) range, which corresponds to only about 5% of the solar energy reaching the Earth's surface. Because of this disadvantage, one strategy that has been adopted to try to improve the performance of titania is to modify this material with metals that have catalytic activity for hydrogen evolution, such as platinum (5).

Platinum is a well-known electrocatalyst for the HER due to the thermodynamic and kinetic aspects of the interaction between hydrogen and platinum atoms (6). Unfortunately, platinum is an expensive and non-abundant metal, which limits its application in the area of hydrogen generation. Although good catalytic performance was achieved for the titania on platinum composite

using platinum nanoparticles (Pt-NPs) with low platinum mass loading, the further decrease in the amount of platinum seems to be detrimental to the catalytic performance (7, 8). Very recently, to try to circumvent the platinum mass loading problem, while maintaining the catalytic performance, a promising approach that has been explored: the deposition of Pt-SAs on the surface of metal oxides such as titania, iron(III) oxide and ceria. Using this approach, it has been possible to obtain high catalytic performance even at ultra-low platinum loadings for Pt-SA-modified titania (9, 10).

Besides titania, Pt-SAs have been used to modify different metal oxides, promoting a significant improvement on the catalytic performance (11, 12). In case of iron(III) oxide, for example, it was verified that Pt-SAs in addition to increasing the performance for photocatalytic hydrogen generation, also improved the stability of the composite material when compared to iron(III) oxide modified with Pt-NPs (13). Following a similar trend, ceria modified with Pt-SAs displayed higher catalytic performance for hydrogen generation when compared to ceria modified with Pt-NPs (14). This high catalytic activity has been attributed to different aspects of the interaction between Pt-SAs and the metal oxide surface, such as the strong metal-support interaction (SMSI), which affects the electronic structure of Pt-SAs and, consequently, their interaction with different types of adsorbates (15). However, in the case of titania, how Pt-SAs affect the energy band structure during illumination is still not well understood.

In this work, we examine the energetic aspects related to the interaction between platinum atoms and titania surface from the synthesis stage of Pt-SAs to their application in photocatalytic experiments, highlighting the role played by oxygen vacancies. These sites determine the saturation of the chemical bonding of the platinum atoms on the surface of the oxide making it more tolerant to the presence of carbon monoxide.

2. Platinum Single Atom Interaction With Metal Oxides

2.1 Study on the Platinum Single Atom Arrangements

An important aspect in understanding the dispersion of single atoms and their efficiency in the photocatalytic reaction remains the clarification of the position of platinum atoms on supporting titania. Numerous studies with metal oxides demonstrate an essential role of defects such as oxygen-vacancies in anchoring platinum atoms where they remain relatively stable (10, 16–22). The deposition process is accompanied with the partial reduction of Pt^{4+} to $Pt^{\delta+}$, which in Kröger-Vink notation, can be written as:

$$(4-\delta)\ Ti'_{Ti} + Pt^{4+} \rightarrow Ti^{x}_{Ti} + Pt^{\delta+} \quad \text{(i)}$$

From this perspective, the control of titania defectivity may play an important role in the amount of platinum facilitated in the form of single atoms. For example, the production of highly defective black titania TiO_{2-x} allowed high dispersity of Pt-SAs up to mass loadings of 0.254% (m/m), having the effect of a large growth in HER and phenol photooxidation for such photocatalyst (17). Another approach in engineering titania surface defects to facilitate the anchoring of platinum atoms involves the incorporation of impurity atoms that reduce the defect formation energy and thus increase their concentration. As demonstrated in the case of trivalent iron, such substitution in the titania structure stabilises Pt-SAs on the surface, in addition to the overall effect of the defective atoms on the semiconductor band gap (18). The role of surface morphology on the deposition of platinum onto titania should be taken into account. Although the presence of platinum atoms was confirmed on the {001} and {101} facets of anatase titania after 'dark deposition' (Section 3.2) (23, 24), photoinduced platinum-precipitation occurs preferentially on the {101} surfaces (25), due to the accumulation of photoexcited electrons from the conduction band (CB) of titania necessary for the reduction of platinum precursor (26).

Another important aspect on the efficiency of Pt-SAs@TiO_2 under operational conditions is the stability of Pt-SAs. In the case of metallic oxides, it has been shown previously that dispersed platinum atoms become mobile and tend to agglomerate at high temperatures (19), in reducing atmosphere (20) or in carbon monoxide oxidation reactions (22). It has been found that UV-photons activate the agglomeration processes of Pt-SAs with formation of more stable Pt-NPs (21). This reaction is accompanied by the reduction of $Pt^{\delta+}$ to Pt^0 observed with X-ray photoelectron spectroscopy (XPS) measurements and apparently related to the photoexcited electron flow taking place during titania illumination. From this point of view, Pt-SAs deposited on the {101} facets of titania could be less stable to agglomeration due to the preferential movement of photoexcited electrons from CB to these surfaces. Strategies to improve the stability

of Pt-SAs include doping of atoms with high electronegativity (such as fluorine) that further interact with the deposited platinum atoms and reduce their mobility (10). Other avenues for the stabilisation of Pt-SAs involve functionalising titania with dopant cationic atoms (18, 27). In addition, it is possible to increase the stability of Pt-SAs by treating the titania substrate in a sodium hydroxide solution before the platinum deposition (10). Finally, the agglomeration rate can be reduced by encapsulating the Pt-SAs and platinum clusters in porous titania (28). The latter, however, limits the turn-over frequency (TOF) during catalysis on encapsulated platinum compared with surface platinum (657.6 h^{-1} *vs.* 1875.7 h^{-1}) in response to reduced access of reactants to the active sites. The possible continuation of this approach could be the use of mesoporous titania-structures derived from metal-oxide-framework to anchor platinum atoms (29). In combination with titania nanotubes, relatively stable platinum atoms were observed even after seven days of HER photocatalysis making the long-term use of atomically dispersed catalyst realistic. There are also attempts of direct impregnation of Pt-SAs inside bulk titania with local formation of platinum(IV) oxide (30). However, it was determined that under relatively mild annealing in reducing environment (hydrogen, 200°C) platinum atoms break the surrounding atomic bounds and come to the surface, with change of platinum charge state from 4+ to δ+.

2.2 Strong Metal-Support Interaction

It is widely known that platinum nanoparticles deposited on metal oxide supports can be subjected to SMSI. This phenomenon manifests itself in the shift of the energy levels of the platinum atoms due to the charge transfer of the metallic particles (31). This alignment in energy leads to the modification of the catalytic properties of platinum toward the oxygen reduction reaction (ORR) and hydrogen oxidation reaction (HOR) (32). It has been observed that the reduction of the size of noble metal particles to single atoms ultimately increases the tolerance of platinum against carbon monoxide adsorption, which, however, essentially depends on the oxidation state of SAs (33). The *ab initio* approach implemented for Pt-SA@TiO_2 after reduction in hydrogen atmosphere predicted carbon monoxide desorption at temperatures above 110 K. This was associated with the coordination saturation of bonds for Pt-SAs with the surrounding atoms and not with their coverage by titania layer, which was also confirmed by low energy ion scattering (15).

2.3 First Principles Studies of Platinum Single Atoms on Titania

To evaluate the energetically more stable configuration, first-principles theoretical considerations of Pt-SAs were performed for ideal (34) and defective structures of anatase-titania (35). Under oxygen-poor conditions (low oxygen partial pressure) the most possible location for platinum-deposition on (101) surface remains the top-most oxygen vacancy due to the lower formation energy (35). However, under oxygen-rich conditions, the deposition site changes to the titanium-surface vacancy. It was also determined that vacancies bind platinum atoms stronger that pristine surface of titania that confirms their leading role in the anchoring of Pt-SAs (36). Density functional theory calculations further showed a double-reduction of the surface Pt-SA located at the oxygen-vacancy as a result of interaction with Ti^{3+}-borne polarons (Ti'_{Ti} in Equation (i)) (37). It has been shown theoretically that the introduction of platinum also leads to the alteration of the electronic structure through formation of platinum states in the bandgap of titania in the case of separated atoms (38), clusters (39, 40) and nanoparticles (41). Due to the spatial localisation of the platinum states near the surface, they represent large trapping sites for conduction band electrons, which can be used for surface reduction reactions. Other studies demonstrated the shift of the *d*-band centre for the platinum atom closer to the Fermi level in defective anatase and rutile titania compared to non-defective titania (42). This shift is often associated with enhanced adsorption of catalytic reagents in the Hammer-Nørskov approach and is proposed to be responsible for enhanced chemisorption of methanol molecules on Pt-SAs.

3. The Effect of Platinum Single Atoms on Photocatalysis and Photoelectrochemical Cell with Metal Oxides

3.1 Physical and Chemical Parameters Influencing the Photocatalysis of Metal Oxides

As a semiconductor material, the photocatalytic behaviour of titania is controlled by the efficiency

of the charge carrier separation process that occurs when the material is illuminated with light of appropriate energy. The charge carrier separation process can be affected by different physicochemical characteristics, such as morphology, crystal structure, surface states, presence of foreign atoms, either in the crystal structure or on the surface of the material (43). Additionally, control of pH is able to modify activity of photocatalyst in liquid environment through the change of the reactant adsorption (44). Due to this wide range of physicochemical parameters affecting the photocatalytic behaviour of titania, it is possible to tune the photoresponse of titania by appropriately adjusting the experimental conditions under which the material is obtained or modified.

3.2 Production Methods for Platinum Metal Oxides

The standard redox potential (E^0) of platinum cations makes its deposition on the titania surface/subsurface a bias-free process. Indeed, E^0 for $[PtCl_6]^{2-}/[PtCl_4]^{2-}$ is 0.68 V (45), while the E_0 for $Ti^{IV}O_2/Ti^{III}OOH$ surface redox is –0.696 V (46). This means that the driving force to reduce $[PtCl_6]^{2-}$ to $[PtCl_4]^{2-}$ is favourable when these species contact a defective titania surface containing Ti^{3+} species. A titania electrode, immersed in platinum-containing solution, develops after a few hours, a new open circuit potential with respect to the initial potential, see **Figure 1**. Due to this, Pt-SAs on the surface/sub-surface of titania can be obtained. Other reported synthesis methods are, for example, photochemical reduction (15, 17, 18, 25, 47–49), dark deposition (9, 10, 21, 50–52), thermal reduction (TR) in hydrogen atmosphere (53–56), TR in atmospheric air (57–59) and methods using advanced techniques (16, 37, 60).

Among the experimental approaches to obtain Pt-SAs, photochemical reduction appears as the preferred method. Typically, in this method, a platinum-containing solution is added to a suspension containing titania powder, then this system is kept under illumination for a certain time. Under such conditions the reduction of $[PtCl_6]^{2-}$ is promoted by electrons photogenerated during illumination of the titania surface. Although this approach has been successfully used to produce Pt-SA on titania, care must be taken in choosing the platinum concentration and light intensity, as it may lead to platinum being deposited as metallic nanoparticles.

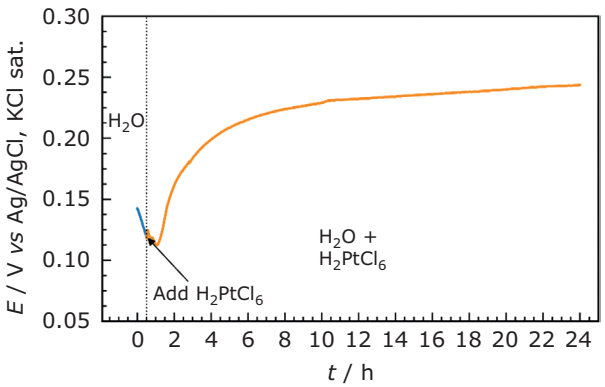

Fig. 1. Monitoring of the open-circuit potential during platinum deposition on a titania electrode (anatase), under dark conditions, with an aqueous solution containing 10 µM hexachloroplatinic acid. The solution after addition of hexachloroplatinic acid was pH 3.9

From an experimental point of view, the 'platinum dark deposition' method is simpler to apply compared to other methods used to synthesise Pt-SAs. It basically consists in immersing a titania electrode in a low-concentration platinum solution under dark conditions and after 24 h the titania electrode is rinsed and dried at relatively low temperature (~70°C). Because it is a site-specific deposition, this method can be used to obtain well-dispersed Pt-SA, which has high photocatalytic activity for HER (50).

The TR methods have some similarities with the dark deposition method. Both methods require an impregnation step in a low-concentration platinum solution, followed by a drying step. The difference is that in case of the TR methods the drying process is carried out at temperature >150°C under a specific atmosphere. TR under hydrogen atmosphere provides a reducing atmosphere to reduce platinum-ions, where hydrogen acts as a reducing agent. In the case of TR in atmospheric air, the reduction of platinum cations can be attributed to electrons released due to the loss of lattice oxygen at the titania surface during the heat treatment (61, 62). Importantly, even at temperatures around 400°C in atmospheric air, it is possible to generate oxygen-vacancies in different polymorphs of titania (63, 64). In case of synthesis using advanced techniques, Pt-SAs has been synthesised through atomic layer deposition (60), electron beam evaporation (37) and vacuum evaporation (16). Using such techniques, it is possible to have a precise control on important aspects of the synthesis, such as reproducibility and platinum loading.

3.3 Ways of Detection of Platinum Single Atoms on Metal Oxides

From a technical point of view, confirming the presence of Pt-SAs on the surface of titania can be challenging and requires sophisticated techniques to differentiate Pt-SAs and metallic platinum nanoparticles (Pt-NPs). The main techniques used to identify and characterise Pt-SAs on the titania surface are high-resolution transmission electron microscopy (HRTEM) (47, 50, 51, 55), X-ray absorption methods (21, 47, 50), XPS (21, 50, 51, 53) and diffuse reflection infrared Fourier transform spectroscopy (DRIFTS) (15, 57, 59). In general, it is necessary to use different techniques to obtain sufficient evidence for the presence of Pt-SAs at titania surface. For example, while HRTEM can be used to identify sub-nanometre species of platinum on the titania surface, as shown in **Figure 2(a)**, spectroscopic techniques such as XPS and X-ray absorption can provide information on the oxidation state of platinum, which helps to distinguish between the presence of Pt-SAs and Pt-NPs. Information on the oxidation state of platinum is a key signature to identify Pt-SAs and Pt-NPs on the titania surface, since Pt-SAs are in an oxidation state between Pt^0 and Pt^{4+} and Pt-NPs are in an oxidation state similar to metallic platinum, as evidenced by X-ray absorption and XPS measurements, **Figure 2(b)** and **2(c)**, respectively.

The change in the electronic state detected by XPS, **Figure 2(c)**, can be attributed to the change in the surface coordination of platinum combined with SMSI with the titania surface. These effects lead to a shift in the binding energy of the 4f orbitals of platinum and the new peaks positions may conform to the 4f orbitals of platinum when in the ionic state, such as $Pt^{\delta+}$ and Pt^{4+} (65).

In addition to XPS and X-ray absorption, DRIFTS is another important technique that can also be used to differentiate Pt-SAs from Pt-NPs. To investigate the nature of platinum sites on titania surface by DRIFTS, carbon monoxide is used as a probe molecule due to its specific adsorption on platinum sites. In this

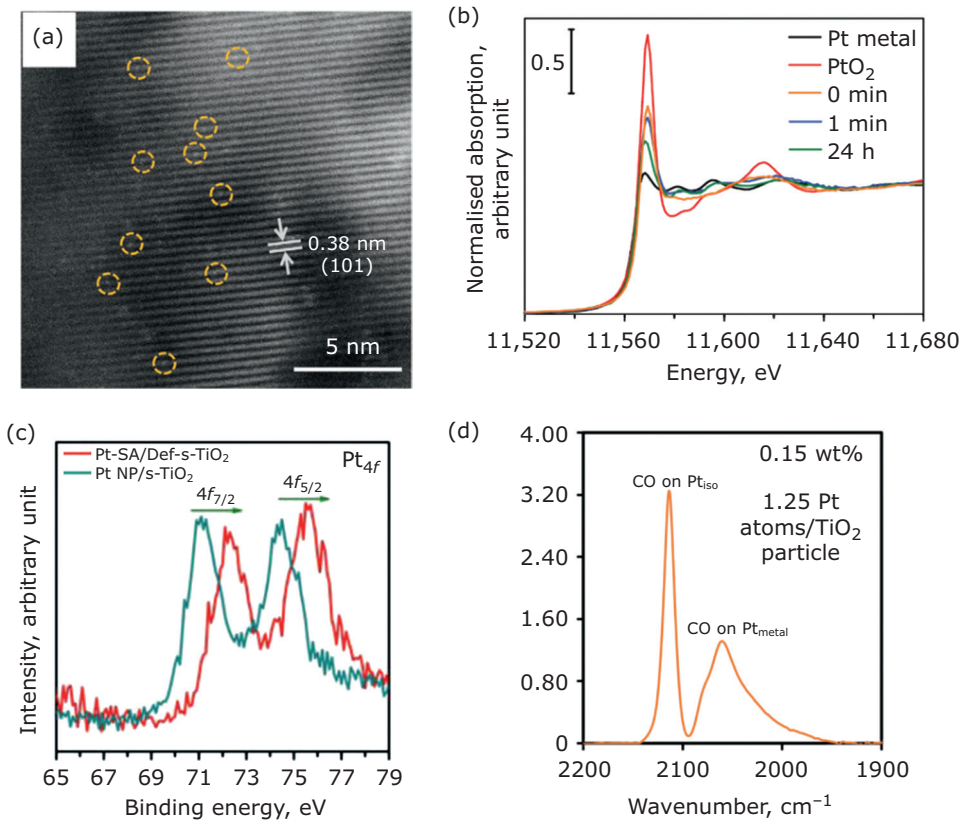

Fig. 2. (a) HRTEM of titania nanotube evidencing the presence of Pt-SAs adapted with permission from (51). Copyright © 2021, John Wiley and Sons; (b) X-ray absorption near edge spectra for platinum dioxide, platinum metal and Pt-SAs on titania surface after different periods of photocatalytic experiments adapted with permission from (21). Copyright © 2022, John Wiley and Sons; (c) XPS results for platinum nanoparticles and Pt-SAs deposited on titania, evidencing the shift in binding energy for platinum 4f orbital in case of Pt-SAs adapted with permission from (53). Copyright © 2021, Elsevier; (d) DRIFTS result for carbon monoxide adsorbed on different platinum species showing characteristic bands for carbon monoxide adsorbed at Pt-SAs and platinum nanoparticles adapted with permission of (59) Copyright © 2017, American Chemical Society

case, when excited with infrared light, the adsorbed carbon monoxide shows different vibrational modes depending on the nature of the platinum site, **Figure 2(d)**. In short, **Figure 2** illustrates a typical set of physicochemical measurements employed to identify and characterise Pt-SAs on titania surface.

3.4 Effect of Platinum Single Atoms on Photocatalysis

Titania is a well-known material for its photoactivity in surface redox reactions first highlighted by Fujishima and Honda in 1972 (66). After absorption by the semiconducting material of a photon with energy above its band gap ($h\nu > E_g$ = 3.2 eV for anatase-titania), photogenerated electrons in CB participate in reduction reactions, while holes in the valence band (VB) oxidise surface adsorbed species **Figure 3(a)**. The main disadvantage of titania as a photocatalyst remains the high recombination rate for the charge carriers, which limits its efficiency (67). The introduction of Pt-NPs allows the separation of carriers by sinking electrons from the titania conduction band to states of platinum

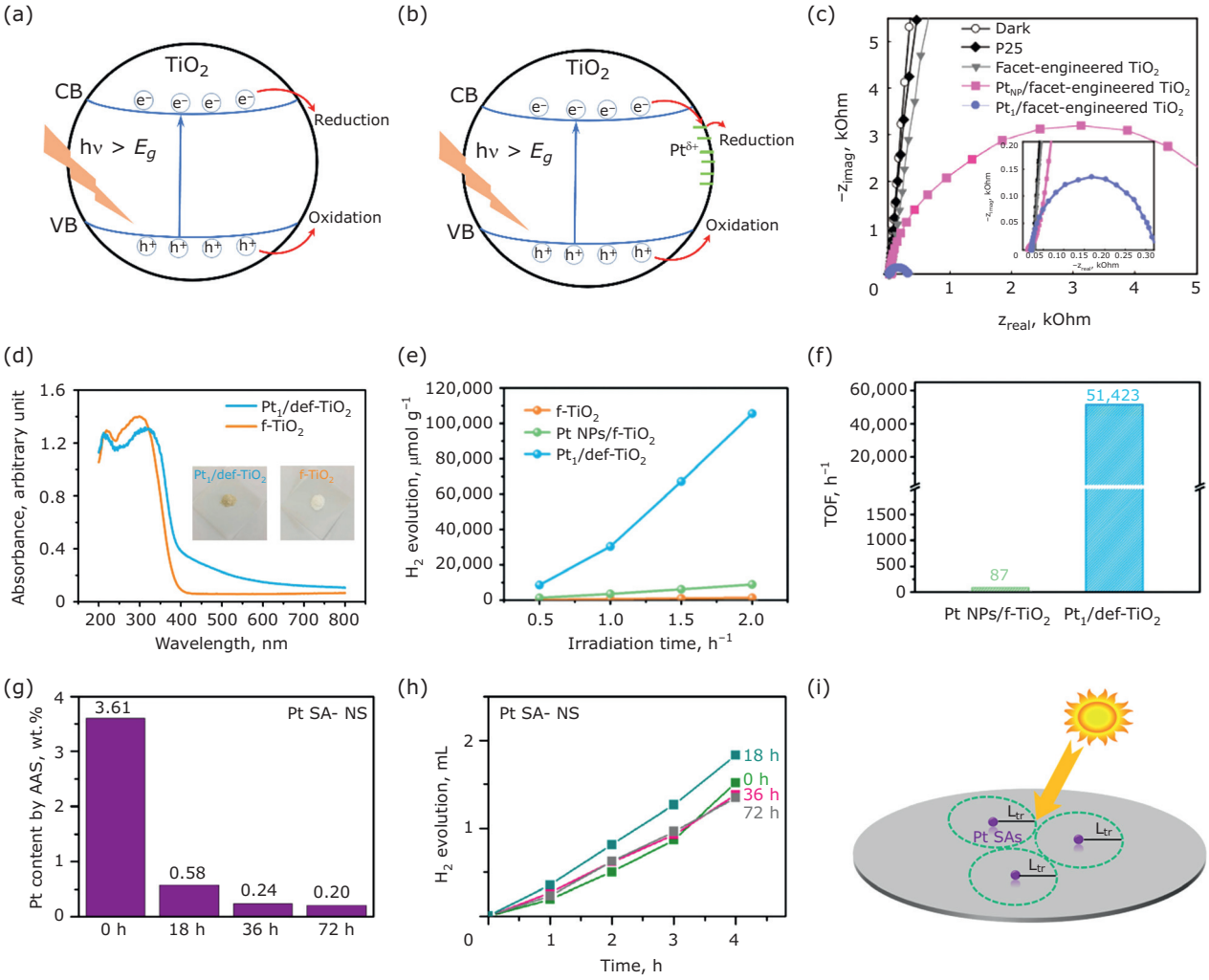

Fig. 3. Effect of Pt-SAs on HER of titania: (a)–(b) schematic energy diagram for platinum-free titania and Pt-SA on titania, respectively; (c) Nyquist plots of various photocatalysts, coated on FTO, from 1 MHz to 0.01 Hz at 0.5 V under solar simulator; the smaller diameter of the semicircle corresponds to the smaller charge transfer resistance, adapted with permission from (48). Copyright © 2021, American Chemical Society; (d) DRS-spectra for Pt-SAs (0.02 wt%) on defective titania (Pt_1/def-TiO_2) and platinum-free titania (f-TiO_2); (e) hydrogen yield; and (f) TOF for Pt_1/def-TiO_2 in comparison with Pt-NPs (0.99 wt%) on f-TiO_2, adapted with permission from (56). Copyright © 2019, John Wiley and Sons; (g) platinum content, measured by electrothermal atomisation atomic absorption spectroscopy (ETA-AAS) analysis; (h) hydrogen-production for the titania-nanosheets decorated with Pt-SAs after sodium cyanide leaching process for the indicated times, adapted with permission from (52). Copyright © 2022, John Wiley and Sons; (i) Optimised schematic configuration of Pt-SAs on surface of semiconducting support, L_{tr} = photoexcited electron diffusion length adapted with permission from (69). Copyright © 2023, American Chemical Society

that can be used for surface reactions (68). Downsizing platinum inclusions to SAs reduces the density of states for platinum atoms and makes the levels discrete, as shown in **Figure 3(b)**. The electron acceptance of the titania CB enables the following scheme, Equations (ii) and (iii), of charge transfer at the surface (52):

$$Pt^{\delta+} + e^- \rightarrow Pt^{(\delta-1)+} \quad \text{(ii)}$$

$$Pt^{(\delta-1)+} + A^+ \rightarrow Pt^{\delta+} + A^0 \quad \text{(iii)}$$

where A is an adsorbed electron-accepting surface species. The introduction of Pt-SAs into titania is accompanied by a decrease in charge transfer resistance compared to pristine titania and Pt-NP on titania, which is usually recorded by semicircles in the Nyquist plot **Figure 3(c)** (23, 48). This predicts a higher rate of charge transfer for photoinduced carriers and their utilisation in redox reactions. The combined effect of semiconductor titania and highly reactive platinum finds its application in photocatalytic HER (9, 10, 21, 23, 25, 50–53, 56, 69, 70). The use of atomically dispersed platinum improves the performance toward hydrogen generation compared to Pt-NPs from 2.5 to 12-fold (9, 10, 50, 53, 56) and up to 600-fold compared to pure titania (52, 53, 56). It should be noted that the anchoring of platinum atoms on the titania surface is related to the formation of additional oxygen vacancies in the oxide in reducing atmosphere (53, 56). The latter is accompanied by additional absorption in the visible range, **Figure 3(d)**, and enhances the hydrogen yield to 52,720 μmol h^{-1} g^{-1} and the turnover frequency to ~51423 h^{-1} (**Figures 3(e)** and **3(f)**), respectively. However, it is observed that only a limited number of surface Pt-SAs participate in the photocatalytic HER, which severely limits the utilisation of atomically dispersed platinum (50–52). For example, the selective removal of highly concentrated platinum atoms from titania surface with sodium cyanide is not accompanied by any significant change in the HER yield, as shown in **Figures 3(g)** and **3(h)** (52). Thus, the limiting factor was attributed to the diffusion length of photogenerated charge carriers in titania, which provides an optimised surface density for Pt-SAs that can accept electrons from the CB **Figure 3(i)** (69). Furthermore, it should be noted that the flat band potential, E_{fb}, of titania is around –0.15 V to –0.4 V *vs.* reversible hydrogen electrode (RHE) over a wide pH range (71, 72). Due to the low difference between E_{fb} and the H^+/H_2 reaction potential (0 V *vs.* RHE), the driving force of photoexcited electrons from CB of titania to realise the photocatalytic HER could also be diminished. For instance, the prominent effect of E_{fb} was observed for differently faceted titania with the loading of Pt-SAs (23). Due to more negative E_{fb}, 001-faceted particles demonstrated a three-fold improvement towards photocatalytic HER compared with 101-faceted titania. Finally, the wide band gap for titania allows utilisation only UV-light in the photocatalysis process, that drastically reduces the sun-driven industrial application of platinum on titania catalysts. From this perspective, band engineering of semiconducting titania may be important to modulate the efficiency of Pt-SAs. In addition to HER, Pt-SAs on titania have been used for other photocatalytic redox reactions (18, 48, 55, 58, 73–76). They are summarised in **Table I**.

4. Summary and Outlook

In summary, we have reviewed recent achievements in the use of Pt-SAs on titania for photocatalytic and photoelectrochemical applications. The general features of the platinum-titania interaction, such as the essential role of oxygen vacancies in the emplacement of platinum atoms on the oxide and the strong metal-support interaction, are highlighted. The synthesis methods of atomically dispersed platinum as well as the driving force for deposition of platinum have been named and discussed. Approaches for theoretical and experimental characterisation of Pt-SAs on titania have been revised. Pt-SAs on titania show enhancement towards photocatalytic HER, compared to Pt-NPs on titania and pure titania. However, it has been shown experimentally that HER on platinum on titania is conditioned only by a low amount of SAs, which dictates the need to improve titania as a light-absorbing material. Multiple experiments with other photocatalytic reactions also demonstrate the advantage of the Pt-SAs on titania photocatalyst over nanoparticulated platinum or pristine titania, which is accompanied by a high selectivity above 90% towards specific products. In addition, the saturation of the chemical bonding for platinum atoms on the oxide surface increases the tolerance to specific poisonous agents, such as carbon monoxide (Section 2.2). This makes the inactivation problem for Pt-SAs less noticeable compared to Pt-NPs and increases the potential use of these catalysts for various applications. However, the existing gaps in understanding the role of Pt-SAs in catalysis point the direction for future studies. Atomically dispersed platinum on the support

Table I Photocatalytic redox reactions performed with Platinum Single Atoms on Titania

Ref.	Type of photocatalyst	Type of photocatalytic experiment	Light source / Intensity	Results
(18)	Photodeposited Pt on TiO_2 and Fe-TiO_2, prepared by sol-gel	Photodegradation of acid orange 7	365 nm UV-LED / 22 mW cm^{-2}	~50% and ~9-fold improvement of photocatalysis for Pt-doped TiO_2 and Fe-TiO_2, respectively
(48)	Pt-SAs at Facet-engineered A-TiO_2	Sulfamethoxazole (SMX), dichloro-phenoxy-acetic acid (2,4-D)	AM 1.5G solar simulator/100 mW cm^{-2}	3.5-fold increase for SMX degradation for Pt_1/TiO_2 compared with TiO_2; 6.4- and 11.3-fold enhancement for SMX and 2, 4D compared with P25
		Perfluorooctanoic acid (PFOA)	254 nm 5 W-UV lamp / 7.87 mW cm^{-2}	15-fold increase of degradation compared with Pt-NPs @ TiO_2
(55)	Dark deposited Pt-SAs on mesoporous TiO_2	Toluene photodegradation	2.5 W VUV mercury lamp (254 nm + 184 nm)	Up to 5.94-fold enhancement in the toluene removal
(58)	Impregnated Pt-SAs in mesoporous TiO_2-spheres	Oxidation of benzyl alcohol	300 W Xe-lamp with 420 nm cut-off filter	3-times higher benzaldehyde yield for 1% Pt/TiO_2 compared with pure TiO_2
(73)	Electrochemically deposited Pt-Au on reduced (R-) TiO_2 NTs	CO_2 reduction	365 nm LED array / 0.208 W cm^{-2}	Pt-Au/R-TiO_2 show 5.5- and 149-fold higher activity compared with Pt-Au/TiO_2 and R-TiO_2, respectively
(74)	Pt-SAs/TiO_2-Ti_3C_2	CO_2 reduction	300 W Xe-lamp with an AM1.5G filter	CO_2-to-CO conversion activity of 20.5 μmol g^{-1} h^{-1} with selectivity 96%; ~5 times higher conversion than that for TiO_2-P25
(75)	Thermal-deposited atomically dispersed Pt on TiO_2-nanosheets	Gas-phase photodegradation of acetaldehyde	400 W Xe-lamp / 80 mW cm^{-2}	~3- and ~7.5-fold higher degradation rate of acetaldehyde for Pt-SAs/TiO_2 against Pt-NPs/TiO_2 and TiO_2, respectively
(76)	Pt-SAs on TiO_2-P25	Acetone conversion to 2,5-hexanedione (HDN) and H_2	300 W Xe-lamp / ~800 mW cm^{-2}	HDN[a] yield 3.87 mmol g^{-1} h^{-1} with selectivity ~93% for Pt-SAs/TiO_2; >13 times higher production than with Ir-, Rh-, Ru-SAs/TiO_2

[a]HDN: 2,5-hexanedione

exhibits a unique electronic structure that alters the thermodynamics of the catalytic steps and thus influences the pathways of the reactions (77). Furthermore, stabilisation of Pt-SAs and prevention of their agglomeration during photocatalysis remains a problem despite recent achievements in this field (Section 2.1). The resolution of these challenges, together with the improvement of titania as a light absorbing material, may provide a deeper insight into the overall catalysis process and become a starting point for the large industrial utilisation of Pt-SAs on titania as photocatalyst.

Acknowledgement

The authors acknowledge financial support from the European Union (ERDF) 'Région Nouvelle Aquitaine'. C. A. G. Bezerra and D. Mamedov thank the Coordenação de Aperfeiçoamento de Pessoal de Nível Superior, Brasil (CAPES) – Finance Code 001 and COOL LONGBOAT (Research Council of Norway - #309827) grants, respectively, for financial support.

References

1. Y. Wang, D. He, H. Chen, D. Wang, *J. Photochem. Photobiol. C: Photochem. Rev.*, 2019, **40**, 117
2. Y. Lan, Y. Lu, Z. Ren, *Nano Energy*, 2013, **2**, (5), 1031
3. E. V. Shkol'nikov, *Russ. J. Phys. Chem. A*, 2016, **90**, (3), 567
4. D. Reyes-Coronado, G. Rodríguez-Gattorno, M. E. Espinosa-Pesqueira, C. Cab, R. de Coss, G. Oskam, *Nanotechnology*, 2008, **19**, (14), 145605

5. V. Kumaravel, S. Mathew, J. Bartlett, S. C. Pillai, *Appl. Catal. B: Environ.*, 2019, **244**, 1021
6. L. A. Kibler, *ChemPhysChem*, 2006, **7**, (5), 985
7. R. Ravi, A. K. Golder, *Coll. Surf. A: Physicochem. Eng. Asp.*, 2023, **663**, 131034
8. Y. Shiraishi, D. Tsukamoto, Y. Sugano, A. Shiro, S. Ichikawa, S. Tanaka, T. Hirai, *ACS Catal.*, 2012, **2**, (9), 1984
9. G. Cha, A. Mazare, I. Hwang, N. Denisov, J. Will, T. Yokosawa, Z. Badura, G. Zoppellaro, A. B. Tesler, E. Spiecker, P. Schmuki, *Electrochim. Acta*, 2022, **412**, 140129
10. S.-M. Wu, I. Hwang, B. Osuagwu, J. Will, Z. Wu, B. B. Sarma, F.-F. Pu, L.-Y. Wang, Z. Badura, G. Zoppellaro, E. Spiecker, P. Schmuki, *ACS Catal.*, 2023, **13**, (1), 33
11. L. Kuai, S. Liu, S. Cao, Y. Ren, E. Kan, Y. Zhao, N. Yu, F. Li, X. Li, Z. Wu, X. Wang, B. Geng, *Chem. Mater.*, 2018, **30**, (16), 5534
12. Q. Tao, J. Song, N. Sun, Y. Ren, L. Xiang, S. Liu, L. Kuai, *Inorg. Chem.*, 2022, **61**, (30), 11932
13. V. Dao, L. A. Cipriano, S.-W. Ki, S. Yadav, W. Wang, G. Di Liberto, K. Chen, H. Son, J.-K. Yang, G. Pacchioni, I.-H. Lee, *Appl. Catal. B: Environ.*, 2023, **330**, 122586
14. L.-N. Chen, K.-P. Hou, Y.-S. Liu, Z.-Y. Qi, Q. Zheng, Y.-H. Lu, J.-Y. Chen, J.-L. Chen, C.-W. Pao, S.-B. Wang, Y.-B. Li, S.-H. Xie, F.-D. Liu, D. Prendergast, L. E. Klebanoff, V. Stavila, M. D. Allendorf, J. Guo, L.-S. Zheng, J. Su, G. A. Somorjai, *J. Am. Chem. Soc.*, 2019, **141**, (45), 17995
15. B. Han, Y. Guo, Y. Huang, W. Xi, J. Xu, J. Luo, H. Qi, Y. Ren, X. Liu, B. Qiao, T. Zhang, *Angew. Chem. Int. Ed.*, 2020, **59**, (29), 11824
16. T.-Y. Chang, Y. Tanaka, R. Ishikawa, K. Toyoura, K. Matsunaga, Y. Ikuhara, N. Shibata, *Nano Lett.*, 2014, **14**, (1), 134
17. T. Wang, Y. Zhu, Z. Luo, Y. Li, J. Niu, C. Wang, *Environ. Chem. Lett.*, 2021, **19**, (2), 1815
18. X. Ma, D. Wang, J. Wu, B. Zhao, F. Chen, *ChemPhysChem*, 2023, **24**, (7), e202200505
19. J. Jones, H. Xiong, A. T. DeLaRiva, E. J. Peterson, H. Pham, S. R. Challa, G. Qi, S. Oh, M. H. Wiebenga, X. I. Pereira Hernández, Y. Wang, A. K. Datye, *Science*, 2016, **353**, (6295), 150
20. X. Li, X. I. Pereira-Hernández, Y. Chen, J. Xu, J. Zhao, C.-W. Pao, C.-Y. Fang, J. Zeng, Y. Wang, B. C. Gates, J. Liu, *Nature*, 2022, **611**, (7935), 284
21. N. Denisov, S. Qin, J. Will, B. N. Vasiljevic, N. V. Skorodumova, I. A. Pašti, B. B. Sarma, B. Osuagwu, T. Yokosawa, J. Voss, J. Wirth, E. Spiecker, P. Schmuki, *Adv. Mater.*, 2023, **35**, (5), 2206569
22. L. Liu, D. M. Meira, R. Arenal, P. Concepcion, A. V. Puga, A. Corma, *ACS Catal.*, 2019, **9**, (12), 10626
23. T. Wei, Y. Zhu, Y. Wu, X. An, L.-M. Liu, *Langmuir*, 2019, **35**, (2), 391
24. T. Wei, P. Ding, T. Wang, L.-M. Liu, X. An, X. Yu, *ACS Catal.*, 2021, **11**, (23), 14669
25. Y. Sui, S. Liu, T. Li, Q. Liu, T. Jiang, Y. Guo, J.-L. Luo, *J. Catal.*, 2017, **353**, 250
26. T. Tachikawa, N. Wang, S. Yamashita, S.-C. Cui, T. Majima, *Angew. Chem. Int. Ed.*, 2010, **49**, (46), 8593
27. J. Chen, M. Jiang, W. Xu, J. Chen, Z. Hong, H. Jia, *Appl. Catal. B: Environ.*, 2019, **259**, 118013
28. H. Wu, X. Yang, S. Zhao, L. Zhai, G. Wang, B. Zhang, Y. Qin, *Chem. Commun.*, 2022, **58**, (8), 1191
29. S. Qin, J. Guo, X. Chen, R. Cao, N. Denisov, Y.-Y. Song, P. Schmuki, *J. Mater. Chem. A*, 2023, **11**, (33), 17759
30. A. A. Ayele, M.-C. Tsai, D. B. Adam, Y. A. Awoke, W.-H. Huang, C.-Y. Chang, S.-C. Liao, P.-Y. Huang, J.-L. Chen, C.-W. Pao, W.-N. Su, B. J. Hwang, *Appl. Catal. A: Gen.*, 2022, **646**, 118861
31. A. Lewera, L. Timperman, A. Roguska, N. Alonso-Vante, *J. Phys. Chem. C*, 2011, **115**, (41), 20153
32. L. Timperman, N. Alonso-Vante, *Electrocatalysis*, 2011, **2**, (3), 181
33. L. DeRita, J. Resasco, S. Dai, A. Boubnov, H. V. Thang, A. S. Hoffman, I. Ro, G. W. Graham, S. R. Bare, G. Pacchioni, X. Pan, P. Christopher, *Nat. Mater.*, 2019, **18**, (7), 746
34. T. Wang, S. Qiu, Z. Dai, R. Hocking, C. Sun, *Appl. Surf. Sci.*, 2020, **533**, 147362
35. X. Wang, L. Zhang, Y. Bu, W. Sun, *Appl. Surf. Sci.*, 2021, **540**, (2), 148357
36. N. Humphrey, S. Bac, S. M. Sharada, *J. Phys. Chem. C*, 2020, **124**, (44), 24187
37. P. Sombut, L. Puntscher, M. Atzmueller, Z. Jakub, M. Reticcioli, M. Meier, G. S. Parkinson, C. Franchini, *Top. Catal.*, 2022, **65**, (17–18), 1620
38. B. Wen, W.-J. Yin, A. Selloni, L.-M. Liu, *Phys. Chem. Chem. Phys.*, 2020, **22**, (19), 10455
39. S. C. Ammal, A. Heyden, *J. Phys. Chem. C*, 2011, **115**, (39), 19246
40. D. Wang, Z.-P. Liu, W.-M. Yang, *ACS Catal.*, 2018, **8**, (8), 7270
41. R. Aso, H. Hojo, Y. Takahashi, T. Akashi, Y. Midoh, F. Ichihashi, H. Nakajima, T. Tamaoka, K. Yubuta, H. Nakanishi, H. Einaga, T. Tanigaki, H. Shinada, Y. Murakami, *Science*, 2022, **378**, (6616), 202
42. Y. Zhang, Y. Wang, K. Su, F. Wang, *J. Mol. Model.*, 2022, **28**, (6), 175
43. J. Schneider, M. Matsuoka, M. Takeuchi, J. Zhang, Y. Horiuchi, M. Anpo, D. W. Bahnemann, *Chem. Rev.*, 2014, **114**, (19), 9919

44. D. Mamedov, S. Zh. Karazhanov, N. Alonso-Vante, *J. Electrochem. Soc.*, 2023, **170**, (5), 056503
45. W. M. Haynes, "CRC Handbook of Chemistry and Physics", eds. W. M. Haynes, D. R. Lide, T. J. Bruno, 97th Edn., Taylor and Francis LLC, Boca Raton, USA, 2016, 2670 pp
46. N. Makivić, J.-Y. Cho, K. D. Harris, J.-M. Tarascon, B. Limoges, V. Balland, *Chem. Mater.*, 2021, **33**, (9), 3436
47. W. He, X. Zhang, K. Zheng, C. Wu, Y. Pan, H. Li, L. Xu, R. Xu, W. Chen, Y. Liu, C. Wang, Z. Sun, S. Wei, *Angew. Chemie Int. Ed.*, 2023, **62**, (2), e202213365
48. S. Weon, M.-J. Suh, C. Chu, D. Huang, E. Stavitski, J.-H. Kim, *ACS EST Engg.*, 2021, **1**, (3), 512
49. J. Wu, X. Ma, L. Xu, B. Zhao, F. Chen, *Appl. Surf. Sci.*, 2019, **489**, 510
50. S. Qin, N. Denisov, B. B. Sarma, I. Hwang, D. E. Doronkin, O. Tomanec, S. Kment, P. Schmuki, *Adv. Mater. Interfaces*, 2022, **9**, (22), 2200808
51. Z. Wu, I. Hwang, G. Cha, S. Qin, O. Tomanec, Z. Badura, S. Kment, R. Zboril, P. Schmuki, *Small*, 2022, **18**, (2), 1, 2104892
52. S. Qin, N. Denisov, J. Will, J. Kolařík, E. Spiecker, P. Schmuki, *Solar RRL*, 2022, **6**, (6), 2101026
53. X. Hu, J. Song, J. Luo, H. Zhang, Z. Sun, C. Li, S. Zheng, Q. Liu, *J. Energy Chem.*, 2021, **62**, 1
54. L. Piccolo, P. Afanasiev, F. Morfin, T. Len, C. Dessal, J. L. Rousset, M. Aouine, F. Bourgain, A. Aguilar-Tapia, O. Proux, Y. Chen, L. Soler, J. Llorca, *ACS Catal.*, 2020, **10**, (21), 12696
55. T. Xu, H. Zheng, P. Zhang, *J. Hazard. Mater.*, 2020, **388**, 121746
56. Y. Chen, S. Ji, W. Sun, Y. Lei, Q. Wang, A. Li, W. Chen, G. Zhou, Z. Zhang, Y. Wang, L. Zheng, Q. Zhang, L. Gu, X. Han, D. Wang, Y. Li, *Angew. Chem. Int. Ed.*, 2020, **59**, (3), 1295
57. H. V. Thang, G. Pacchioni, L. DeRita, P. Christopher, *J. Catal.*, 2018, **367**, 104
58. N. Sun, J. Song, Q. Tao, E. Kan, L. Kuai, *Micropor. Mesopor. Mater.*, 2022, **337**, 111949
59. L. DeRita, S. Dai, K. Lopez-Zepeda, N. Pham, G. W. Graham, X. Pan, P. Christopher, *J. Am. Chem. Soc.*, 2017, **139**, (40), 14150
60. Z. Tian, Y. Da, M. Wang, X. Dou, X. Cui, J. Chen, R. Jiang, S. Xi, B. Cui, Y. Luo, H. Yang, Y. Long, Y. Xiao, W. Chen, *Nat. Commun.*, 2023, **14**, 142
61. K. Komaguchi, T. Maruoka, H. Nakano, I. Imae, Y. Ooyama, Y. Harima, *J. Phys. Chem. C*, 2010, **114**, (2), 1240
62. E. Carter, A. F. Carley, D. M. Murphy, *J. Phys. Chem. C*, 2007, **111**, (28), 10630
63. C. A. G. Bezerra, J. P. T. da S. Santos, G. G. Bessegato, C. L. de Paiva e Silva Zanta, V. Del Colle, G. Tremiliosi-Filho, *Electrochim. Acta*, 2022, **404**, 139712
64. D. Zhao, X. Zhang, W. Wang, L. Sui, C. Guo, Y. Xu, X. Zhou, X. Cheng, S. Gao, L. Huo, *Sensors Actuators B: Chem.*, 2022, **370**, 132423
65. S. Hejazi, S. Mohajernia, B. Osuagwu, G. Zoppellaro, P. Andryskova, O. Tomanec, S. Kment, R. Zbořil, P. Schmuki, *Adv. Mater.*, 2020, **32**, (16), 1908505
66. A. Fujishima, K. Honda, *Nature*, 1972, **238**, (5358), 37
67. J. Low, J. Yu, M. Jaroniec, S. Wageh, A. A. Al-Ghamdi, *Adv. Mater.*, 2017, **29**, (20), 1601694
68. A. Naldoni, M. D'Arienzo, M. Altomare, M. Marelli, R. Scotti, F. Morazzoni, E. Selli, V. Dal Santo, *Appl. Catal. B: Environ.*, 2013, **130**–**131**, 239
69. S. Qin, J. Will, H. Kim, N. Denisov, S. Carl, E. Spiecker, P. Schmuki, *ACS Energy Lett.*, 2023, **8**, (2), 1209
70. J. Xi, X. Zhang, X. Zhou, X. Wu, S. Wang, W. Yu, N. Yan, K. P. Loh, Q.-H. Xu, *J. Colloid Interface Sci.*, 2022, **623**, 799
71. Y. Matsumoto, T. Yoshikawa, E. Sato, *J. Electrochem. Soc.*, 1989, **136**, (5), 1389
72. M. Radecka, M. Rekas, A. Trenczek-Zajac, K. Zakrzewska, *J. Power Sources*, 2008, **181**, (1), 46
73. H. Pan, X. Wang, Z. Xiong, M. Sun, M. Murugananthan, Y. Zhang, *Environ. Res.*, 2021, **198**, 111176
74. H. Li, Q. Song, S. Wan, C.-W. Tung, C. Liu, Y. Pan, G.-Q. Luo, H. M. Chen, S. Cao, J. Yu, L.-M. Zhang, *Small*, 2023, **19**, (34), 2301711
75. A. Mahmood, X. Wang, X. Xie, J. Sun, *ACS Appl. Nano Mater.*, 2021, **4**, (4), 3799
76. P. Zhou, Y. Chao, F. Lv, K. Wang, W. Zhang, J. Zhou, H. Chen, L. Wang, Y. Li, Q. Zhang, L. Gu, S. Guo, *ACS Catal.*, 2020, **10**, (16), 9109
77. U. Kerketta, A. B. Tesler, P. Schmuki, *Catalysts*, 2022, **12**, (10), 1223

The Authors

Carlos André Gomes Bezerra, PhD, is a postdoctoral fellow at the Université de Poitiers, France. He earned his PhD in Chemistry from the Chemical Institute of São Carlos, University of São Paulo (USP) Brazil, with a thesis focused on the photoelectrooxidation of alcohols using modified titania nanotubes. Prior to his PhD, Bezerra received a BSc in Chemistry from the Universidade Federal do Maranhão, Brazil, and an MSc in Chemistry from the Universidade Federal de São Carlos. His Master's thesis focused on developing new synthetic approaches for nanostructured lithium-ion battery cathodes. His current research project focuses on photoelectrocatalytic materials for energy generation.

Damir Mamedov completed his specialisation in Materials Science and Engineering in 2018 at National Nuclear Research University (MEPhI), Russia. During his PhD programme at MEPhI, he received a fellowship at the Norwegian Institute of Energy Technology, where he developed functional materials for solar cells. Since 2022, Damir has been working as a researcher at the University of Poitiers, France, on semiconducting metal oxides for photocatalytic water splitting. Most of his studies focus on experimental approaches in photocatalysis and photoelectrochemistry. However, Damir is also passionate about *ab initio* theoretical methods.

Nicolas Alonso-Vante is a Professor of Chemistry at Poitiers University. Professor Alonso-Vante's research during the years has been aimed at developing catalyst materials in the nanoscale for electrocatalysis and photoelectrocatalysis. He places key emphasis on engineering catalyst materials at the nano- and atomic-scales to induce desired properties, and then on designing and developing new technologies that employ them in electrified interfacial processes to convert, for example, water into valuable molecular products such as hydrogen in which micro-scale fuel cells and electrolysers serve as a platform. Professor Alonso-Vante is Emeritus since September 2021.